Analysis and Modeling Framework of Common Mode Noise in a Three-phase Motor System

Manish K. Mathew^{#1}, Xin Yan^{#2}, Yuandong Guo^{#3}, Tanner Fokkens^{#4}, Li Shen^{#5}, Daryl Beetner^{#6}, and DongHyun Kim^{#7}

**EMC Laboratory

**Missouri University of Science and Technology

Rolla, MO, USA

1*mkmbzm, 7dkim @mst.edu

Abstract—Electromagnetic interference (EMI) issue is one of the major constraints of power electronic converters, especially for variable-speed systems. In this work, the common mode noise in a three-phase motor system is analyzed and modeled. The three-phase pulse-width modulation (PWM) inverter creates high magnitudes of dv/dt and di/dt, resulting in common mode noise and disturbance power. In this paper, the common mode noise and disturbance power modeling method are proposed for three-phase motor systems. The proposed equivalent circuit model comprises detailed models for insulated gate bipolar transistors (IGBTs), EMI filters, a three-phase motor and a printed circuit board (PCB). The proposed model of a three-phase system was verified by measurement with and without additional Y-capacitors. The measured and modeled common-mode noise shows a correlation in broadband common-mode noise reduction.

Keywords— Three-phase motor system, IGBT, Y-capacitors, common mode noise, disturbance power

I. INTRODUCTION

Electromagnetic interference (EMI) issues are one of the major constraints to the design of power electronic converters, especially for variable-speed systems. Three-phase motors are widely used in a variety of machines, as they have substantial starting torque and power in a small package. Due to the high dv/dt and di/dt magnitudes of the inverter circuit, the three-phase motor system generates common mode noise and disturbance power which may affect other devices.

In literature, several papers show individual circuit component modeling, but system-level modeling for entire the three-phase motor system has never been proposed. The common mode noise in a three-phase motor drive system was modeled in [1] using an equivalent circuit impedance-based estimation. In [2], the asymmetry in parasitic capacitance of motor coils is identified as the root cause of common mode current in a three-phase motor drive system. The switching cells of an inverter in [3] were replaced by current and voltage source models, highlighting the negative effects of stray elements and the importance of motor and cable propagation paths. An EMI characterization of high-power IGBT modules was carried out in [4] by modeling the IGBTs including the internal stray elements. Previous modeling approaches only consider a portion of the complete three-phase motor system thereby limiting the common-mode noise and EMI analysis. In [5], a complete modeling framework was introduced to model the ac-dc power supply in a LED TV for analyzing the conducted emission below

This work was supported in part by the National Science Foundation (NSF) under Grant No. IIP-1916535.

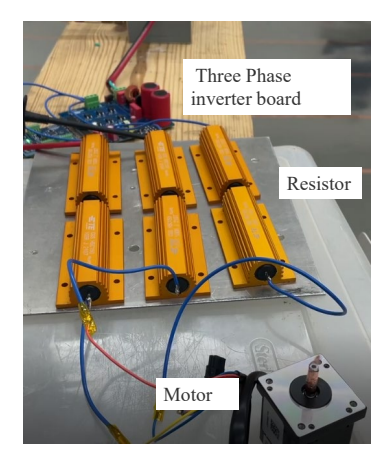


Fig. 1. Three-phase motor system.

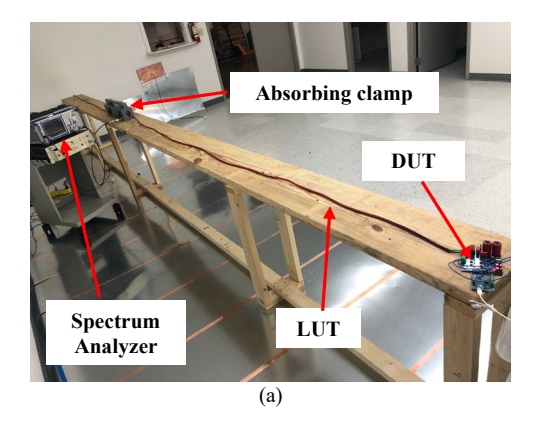
1 MHz. However, such an approach was not used in three-phase motor systems. A complete modeling framework that includes all the circuits of the three-phase motor system can help analyze and help lower the total disturbance power and common mode noise levels.

In this paper, a modeling framework for the three-phase motor system is proposed and verified using measurement results. The parasitic parameters of an insulated gate bipolar transistor (IGBT), EMI filter, three-phase motor, PCB, and RLC components are extracted. The proposed equivalent circuit model of the system is applied to analyze and lower the common mode noise and disturbance power levels.

II. THREE-PHASE MOTOR SYSTEM SETUP

An evaluation board (EVAL-M7-HVIGBT-INV) from Infineon, as shown in Fig. 1, is used in the proposed modeling and analysis. The board requires a 220V input AC and it delivers three-phase 310V outputs. The maximum output power of the board is 200W, thus six 100-ohm power resistors were used to limit the power. The Brushless DC (BLDC) three-phase motor was connected to resistors in series.

The CISPR 16-1-3 standard was adopted to measure the disturbance power from the line under test (LUT). The measurement was carried out as shown in Fig. 2 (a). A 5m long cable was used to power the board and a spectrum analyzer, and an absorbing clamp was used to measure the disturbance power. The disturbance power was measured at 30 sample positions from 10 cm to 510 cm. A quasi-peak detector with max-hold power was set in the spectrum analyzer to measure the



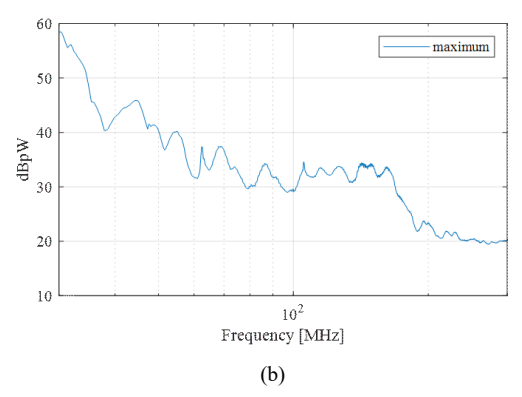


Fig 2. (a) Disturbance power measurement setup. (b) Measurement results.

disturbance power from 30 MHz to 300 MHz. As shown in Fig. 2 (b), the disturbance power from the evaluation board is high and needs to be lowered.

III. PROPOSED MODELLING FRAMEWORK

To analyze the noise generated by the three-phase motor system, IGBT, EMI filter, PCB, and motors are modeled separately. The modeling methods are discussed in this section.

A. Modelling IGBT using Genetic Algorithm

The IGBT on the evaluation board is modeled by an ideal switch with parasitics. Besides the capacitances, the resistances and inductances of the gate, collector, and emitter pins are considered [6]. To build the equivalent circuit model, the first step is a one-port measurement using a vector network analyzer (VNA) from 100 kHz to 1.5 GHz. As shown in Fig. 3 (a), the IGBT is soldered to an open-ended semi-rigid cable, and VNA is connected to the other side of the cable. The measured frequency is from 100 kHz to 1.5 GHz, with a log-scale sweep. The port extension was turned on to calibrate the delay of the cable. Three Z-parameters are tested: collector to emitter, gate to the emitter, and gate to the collector. While the measured pins of the IGBT are soldered to the signal and ground of the cable, respectively, the third unused pin is floating.

Afterward, the genetic algorithm is utilized to create the circuit model of IGBT. The equivalent circuit is shown in Fig. 3 (b). There are 9 unknown variables: R_c , R_g , R_e , L_c , L_g , L_e , C_{gc} , C_{ge} , C_{ce} . Correlating to the Z-parameters measurement

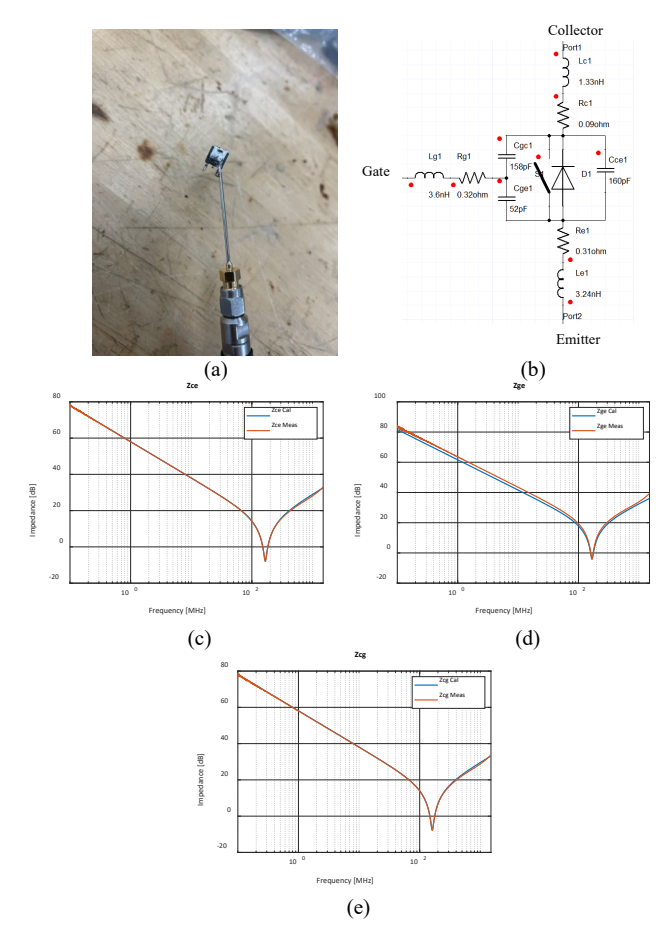


Fig. 3. (a) IGBT soldered to semi-rigid cable. (b) IGBT equivalent circuit. (c) Z_{ce} comparison. (d) Z_{ge} comparison. (e) Z_{cg} comparison.

setups, 3 equations of the impedance is proposed, where all 9 variables are included. The error function in the genetic algorithm is given by:

$$\sum_{i}^{n} \left| \frac{Z_{i,cal} - Z_{i,ref}}{Z_{i,ref}} \right|, \tag{1}$$

where $Z_{i,ref}$ is the measured impedance at frequency point i, $Z_{i,cal}$ is impedance from the genetic algorithm. The total frequency points are n. As the results given by the genetic algorithm could be different each time, to increase the accuracy, the algorithm runs 100 times and the mean values of the 9 variables are calculated and recorded. The comparison of the z-parameters between the measurement and fitting is shown in Fig. 3 (c), (d), &(e). The impedances calculated from the circuit model show a high level of correlation with the measurement results, verifying the proposed IGBT modeling using genetic algorithm. The obtained parasitic values are shown in the

B. EMI Filter Modelling

As shown in Fig. 4 (a), the EMI filter on the board includes a common-mode choke, two of X-capacitors and two of Y-



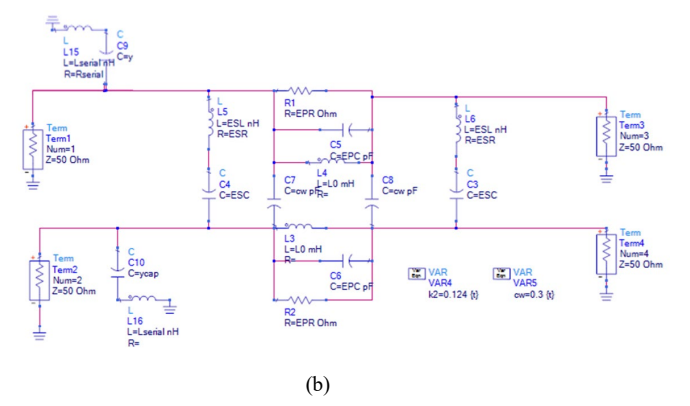


Fig. 4 (a) EMI filter on the PCB. (b) The equivalent circuit of the EMI filter.

capacitors. The modeling strategy of the EMI filter is similar to the [7]. The film capacitors and common mode choke are modeled in a full-wave simulation tool, including differential and common mode responses. For the X-capacitors, similar to common mode chokes, the mutual couplings need to be considered and are modeled using the full-wave 3D simulation tool, CST. Some of the parasitics are fine-tuned based on the measurement results. The equivalent circuit of the EMI filter is shown in Fig.4 (b).

C. Three-phase Motor Modelling

The motor modeling is separated into two parts: low frequency and high frequency. An equivalent circuit for the low-frequency range of 1 Hz to 100 kHz is shown in Fig. 5 (a), based on the impedance measurement results. Fig. 5 (b) and (c) show the comparison between the simulation and measurement of the common mode impedance and differential mode impedance, respectively. The equivalent circuit shows a high level of correlation to the measurement.

For the high-frequency range, from 100 kHz to 300 MHz, the S-parameter is measured, and the SPICE model is converted. Fig. 6 (a) and (b) show the high level of correlation between the measured S-parameter and SPICE model results.

Afterward, the motor SPICE model of the whole frequency range is obtained through the vector fitting process, by combing the low-frequency and high-frequency responses.

The low-frequency range equivalent circuit based on the impedance measurement can be further enhanced by a lower-frequency VNA measurement in the future.

D. PCB SPICE Modelling

The PCB of the evaluation board is simulated using a 3D full-wave simulation tool, ANSYS HFSS. The circuit ports are set at the locations of the components and the s-parameters are

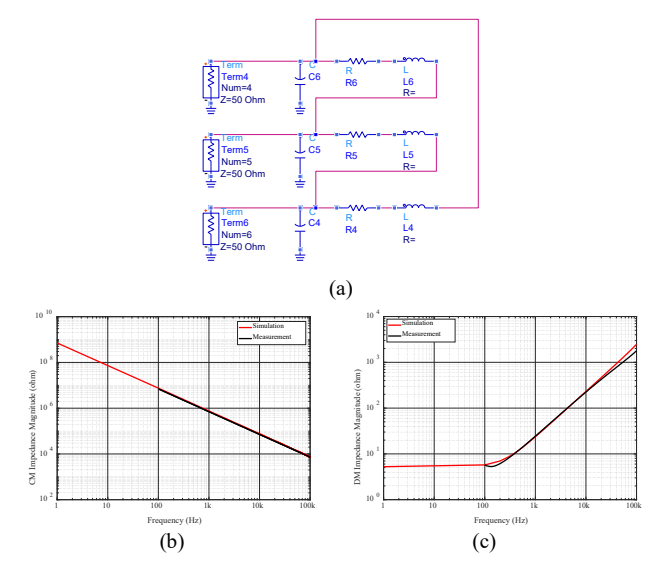


Fig. 5. Low frequency model of the motor. (a) Equivalent circuit. (b) Comparison of the common mode impedance. (c) Comparison of the differential mode impedance.

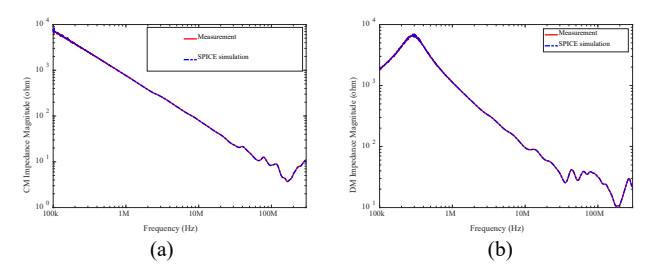


Fig. 6. Comparison between the measured s-parameter and spice model results. (a) common mode (b) differential mode.

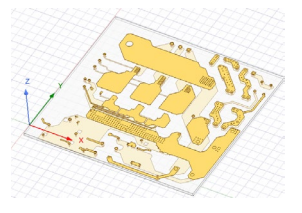


Fig. 7. PCB simulation model in HFSS.

simulated. Then, the simulated s-parameter is converted to a SPICE model. Regarding the common mode current, the capacitance from the PCB to the reference ground is extracted in ANSYS Q3D. The capacitor is added to the circuit model to represent the common mode current path in the three-phase motor system.

IV. VALIDATION

A complete circuit model of the three-phase motor system is represented in Fig. 7(a). The IGBT, EMI filter, motor and PCB models are combined to model the entire system. An ideal

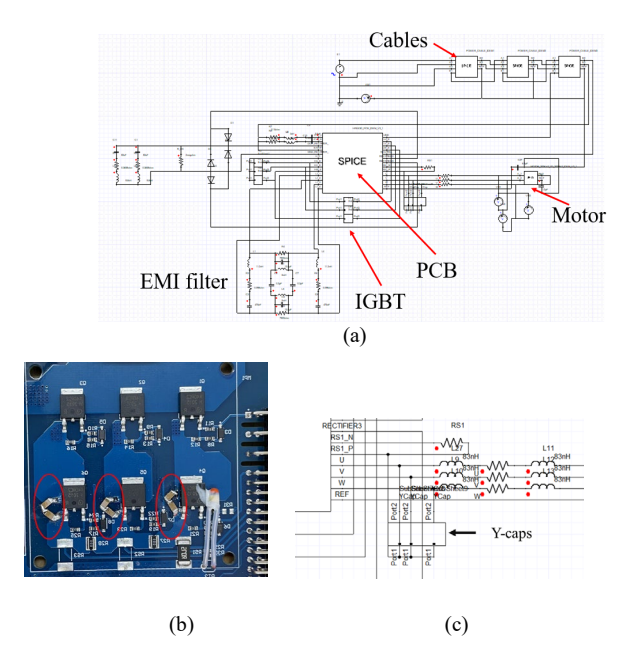


Fig. 7. (a) Proposed circuit model. (b) Add Y-capacitors to the board. (c) Add Y-capacitors in circuit model.

voltage source is provided as an input. The common-mode current is monitored on the return path through the capacitors. To mitigate the common noise, shunt capacitors were added from the three-phase output to the PCB ground (Y-capacitors), as shown in Fig. 7 (b). The measurement results are shown in Fig. 8 (a). It shows that the Y-capacitors can reduce the common mode noise. To validate the circuit model, the Y-capacitors with parasitics are added to the circuit model, as shown in Fig. 7 (c), and the simulation comparison is shown in Fig. 8 (b). A broadband reduction is shown in the simulation. The peak around 4 MHz in simulation results may relate to the quality of the PCB SPICE model and will be further investigated in the future. Both measurement and simulation show a similar trend in the reduction of broadband common mode noise, which verifies that the proposed simulation model can be used to analyze and predict the trend of common mode noise.

V. CONCLUSION

In this work, a complete system modeling framework approach was utilized which includes IGBT equivalent circuit modeling using a genetic algorithm. The EMI filter is modeled using a 3D full-wave simulation tool. The equivalent circuit of the low-frequency three-phase motor is obtained from the impedance measurement and the high-frequency modeling was obtained from S-parameter measurements. The S-parameters from the circuit ports of the evaluation board and the capacitance between the PCB and reference ground are extracted from 3D simulation, as well. Addition of Y- capacitors in both the evaluation board and the proposed model shows similar broadband common mode noise reduction, thereby validating the capability of the model to predict and analyze common mode noise in three-phase motor systems. For future work, an accurate transfer function from common mode current to disturbance

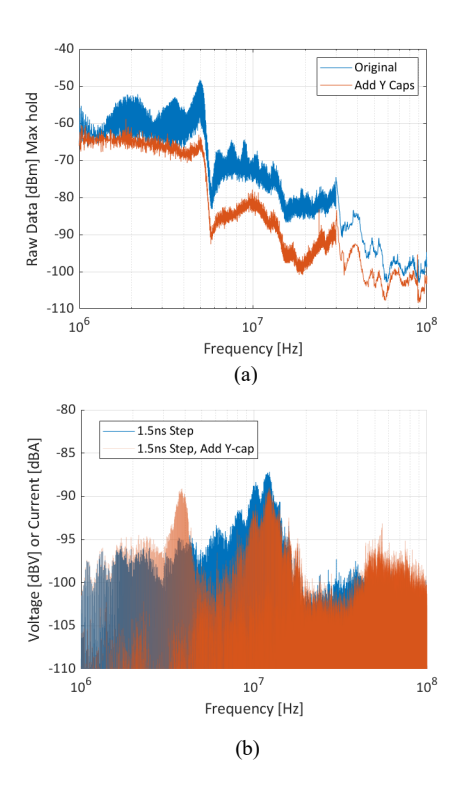


Fig. 8. (a) Measurement comparison (b) Simulation comparison.

power will be used for a direct comparison between measurement and simulation.

REFERENCES

- [1] H. Rathnayake, A. Ganjavi, F. Zare, D. Kumar and P. Davari, "Common-mode noise modelling and resonant estimation in a three-phase motor drive system: 9-150 kHz frequency range," 2020 22nd European Conference on Power Electronics and Applications (EPE'20 ECCE Europe), Lyon, France, 2020, pp. 1-10, doi: 10.23919/EPE20ECCEEurope43536.2020.9215887..
- [2] D. Bellan, "Circuit models for EMC analysis of CM current in three-phase motor drive systems," 2014 6th IEEE Power India International Conference (PIICON), Delhi, India, 2014, pp. 1-5, doi: 10.1109/POWERI.2014.7117718.
- [3] B. Revol, J. Roudet, J. -L. Schanen and P. Loizelet, "EMI Study of Three-Phase Inverter-Fed Motor Drives," in IEEE Transactions on Industry Applications, vol. 47, no. 1, pp. 223-231, Jan.-Feb. 2011, doi: 10.1109/TIA.2010.2091193..
- [4] G. Busatto, C. Abbate, F. Iannuzzo, L. Fratelli, B. Cascone and G. Giannini, "EMI Characterisation of high power IGBT modules for Traction Application," 2005 IEEE 36th Power Electronics Specialists Conference, Dresden, Germany, 2005, pp. 2180-2186, doi: 10.1109/PESC.2005.1581935.C. Wu et al., "Analysis and Modeling of Conducted EMI from an AC–DC Power Supply in LED TV up to 1 MHz," in IEEE Transactions on Electromagnetic Compatibility, vol. 61, no. 6, pp. 2050-2059, Dec. 2019, doi: 10.1109/TEMC.2019.2954360.
- [5] Y. S. Cao, Y. Wang, L. Jiang, A. E. Ruehli, J. Fan and J. L. Drewniak, "Quantifying EMI: A Methodology for Determining and Quantifying Radiation for Practical Design Guidelines," in *IEEE Trans. on Electromagnetic Compatibility*, vol. 59, no. 5, pp. 1424-1432, Oct. 2017
- [6] J. Wang and W. Chen, "A New Method to Measure the Parasitic Parameter Model of IGBT on Bias Voltage," in *IEEE Transactions on Electron Devices*, vol. 68, no. 5, pp. 2387-2394, May 2021, doi: 10.1109/TED.2021.3068087.
- [7] R. He et al., "Modeling Strategy for EMI Filters," in *IEEE Transactions on Electromagnetic Compatibility*, vol. 62, no. 4, pp. 1572-1581, Aug. 2020, doi: 10.1109/TEMC.2020.3006127.